

LIMITATIONS FOR ACCELERATION OF INTERMEDIATE MASS PARTICLES WITH TRAVELLING WAVE STRUCTURE

V. Paramonov *, INR of the RAS, Moscow, 117312, Russia

Abstract

The Disk Loaded Waveguide (DLW) is the mostly used high frequency structure for acceleration of lightweight particles - electrons in the high energy range. DLW parameters are considered for the lower frequency range and lower particle velocity. Physical and technical restrictions for DLW application for the low particles velocity are analyzed. Basing on particularities of acceleration with travelling wave, deep optimization of DLW cells dimensions, the choice of optimal operating phase advance for each DLW section and combination of forward and backward wave modes, it looks possible to create the simple, cost effective acceleration system for intermediate particles acceleration in the moderate velocity range, in some parameters overcoming accelerating system with RF cavities in the standing wave mode.

INTRODUCTION

Due to relative simplicity of manufacturing and sufficient RF efficiency DLW is widely used for acceleration of electrons with $\beta \approx 1$ and the structure is well studied for this case. But the same features stimulate consideration of DLW application for acceleration of more heavy particles - muons and protons. For this task DLW parameters should be considered for lower β and for different modes of operation to define the technical and the physical limitations for DLW application.

DLW PARAMETERS

The distribution of the longitudinal electric field E_z in the DLW aperture for Travelling Wave (TW) operation is the sum over spatial harmonics, [1]:

$$E_z(r, z) = \sum_{-\infty}^{+\infty} E_n I_0(k_{sn} r) e^{-ik_{zn} z}, k_{zn} = \frac{\theta + 2n\pi}{d_p}, \quad (1)$$

$$k_{sn}^2 = k_{zn}^2 - k^2, k = \frac{2\pi}{\lambda},$$

$$d_p = \frac{\beta\lambda\theta}{2\pi}, n = 0, \quad d_p = \left| \frac{\beta\lambda(\theta - 2\pi)}{2\pi} \right|, n = -1.$$

where E_n is the amplitude of the n -th spatial harmonic, $I_0(k_{sn} r)$ is the modified Bessel function, λ and θ are the operating wavelength and the operating phase advance, β is the particle velocity. The length of the cell d_p is defined from the synchronism with appropriate spatial harmonic. Usually the main harmonic $n = 0$ is used for acceleration. This case DLW has a positive dispersion and operates in

Forward Wave (FW) TW mode. Acceleration with the first nearest spatial harmonic $n = -1$ is also possible. There are a lot of papers with proposals, but for $\beta \sim 1$ it loses in RF efficiency, because $|E_0| > |E_{-1}|$. Until now just one practical application, using DLW with the first harmonic $n = -1$ is known with the interesting results for particles focusing, [2]. Such case DLW operates in Backward Wave (BW) TW mode and has a negative dispersion.

Parameters of the DLW structure were calculated and

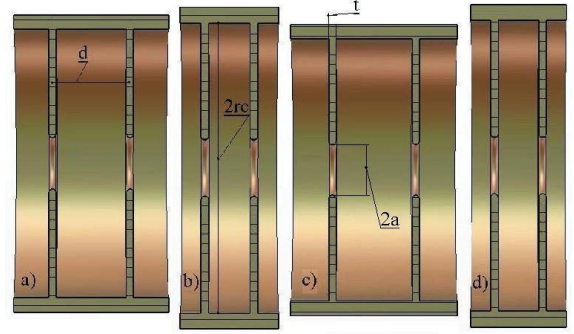


Figure 1: The DLW geometry for FW operation $\beta = 0.90, \theta = 90^\circ$, (a), $\beta = 0.41, \theta = 120^\circ$, (b) and BW operation, $\beta = 0.41, \theta = 120^\circ$, (c), $\beta = 0.20, \theta = 120^\circ$, (d).

stored in the data library in the same procedure, as described in [3] by using fast and precise 2D FEM codes. Examples of the considered shapes of DLW cells are shown in Fig. 1 for different β and θ combinations. For more details of the data library storage see [4]. Simulations of the DLW parameters were performed assuming the L-band operating frequency $f_0 = 1296 MHz$ and for another f_0 value parameters can be recalculated by using well known scaling relations.

The magnitude of the n -th spatial harmonic E_n is related with the flux of RF power P_t as:

$$\frac{E_n}{\sqrt{P_t}} = \sqrt{\frac{2\pi Z_{en}}{\lambda|\beta_g|Q}} \sim f_0, \quad (2)$$

$$Z_{en} = \frac{|\int_{d_p} E_z(0, z) e^{ik_{zn} z} dz|^2}{P_s d_p} \sim f_0^{\frac{1}{2}},$$

$$\alpha = \frac{\pi}{\lambda|\beta_g|Q} \sim f_0^{\frac{3}{2}},$$

where Z_{en} is the value of the effective shunt impedance per unit of length for the n -th harmonic, P_s is the power of RF losses in the cell surface and α is the attenuation.

The main parameter for the DLW structure is the group velocity β_g , which depends mainly on the aperture radius a

* paramono@inr.ru

and θ . In Fig. 2 are shown the calculated surfaces $\beta_g(\frac{a}{\lambda}, \theta)$ for different β both for FW and BW operation, where t is the iris thickness. Both for FW and BW operation for $a = const$ one can see sin-like dependence β_g on θ for all β values. For the fixed θ there is a fast rise $\beta_g \sim a^3$ with aperture increasing.

In Fig. 3 are shown the calculated surfaces for quality fac-

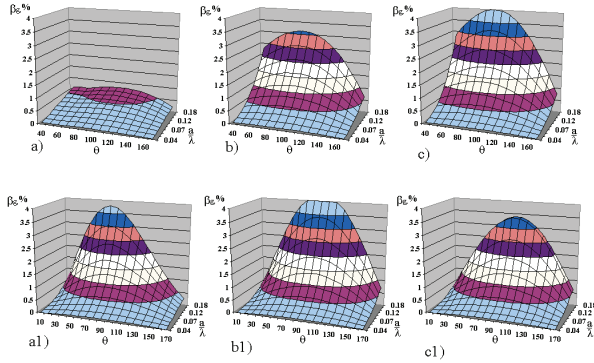


Figure 2: The surfaces $\beta_g(\frac{a}{\lambda}, \theta)$ for $\beta = 0.22$ (a,a1), $\beta = 0.57$ (b,b1) and $\beta = 0.92$ (c,c1). The line (a,b,c) is for $n = 0$ and the line (a1,b1,c1) is $n = -1, t = 5mm$

tor $Q(\frac{a}{\lambda}, \theta)$ for different β both for FW and BW operation. The DLW operates in TM_{01} - wave and the main parameter, which defines Q value is the ratio of the cell length to the cell radius. As one can see from the surfaces in Fig. 3, there are no essential Q dependence on the aperture radius a . For lower β values quality factor decreases, especially for FW operation. With θ decreasing the cell length decreases for FW operation and increases for BW one. It explains the opposite slope of surfaces in Fig. 3 for forward and backward waves. For synchronous harmonic $n = -1$ the cell length is all time larger, than for synchronous harmonic $n = 0$ and quality factor is higher all time. It results in lower wave attenuation for BW operation.

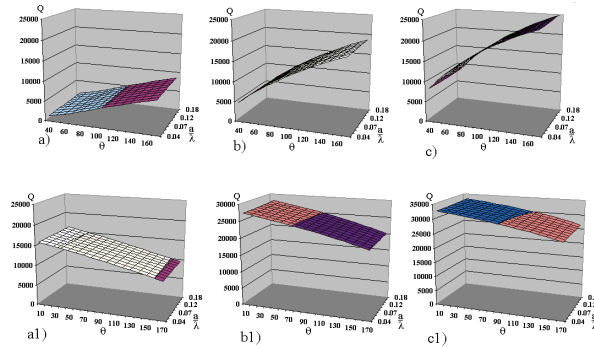


Figure 3: The surfaces $Q(\frac{a}{\lambda}, \theta)$ for $\beta = 0.22$ (a,a1), $\beta = 0.57$ (b,b1) and $\beta = 0.92$ (c,c1). The line (a,b,c) is for $n = 0$ and the line (a1,b1,c1) is $n = -1, t = 5mm$

PARAMETERS AND LIMITATIONS

DLW application for very low $\beta \leq 0.2$ is limited by natural field decay from aperture $r = a$ to axis $r = 0$. In Fig. 4a are shown E_z distribution along r for different β values at the distance $\frac{d_p}{3}$ from the iris center. For FW $n = 0$ operation, with the overestimation near (15 – 20)%, E_0 value can be estimated as, [4]:

$$\frac{E_0}{\sqrt{P_t}} \approx 100 \frac{F(a, \lambda, \beta)}{\lambda \sqrt{|\beta_g|}}, \quad (3)$$

$$F(a, \lambda, \beta) = I_0 \left(\frac{2\pi a \sqrt{1 - \beta^2}}{\beta \lambda} \right),$$

where the function $F(a, \lambda, \beta)$ describes this field decay. The plot $F(a, \lambda, \beta)$ is shown in Fig. 4b. The maximal field value E_{max} takes place at the iris tips. Together with E_0 reduction for the fixed P_t value we get the strong $\frac{E_{max}}{E_0}$ increasing for low β . The effect of field decay is common

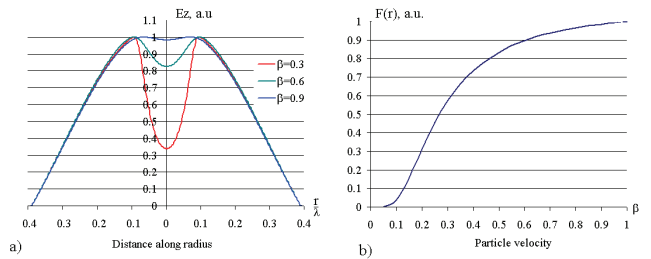


Figure 4: E_z distribution along r for different β value, (a), and the plot of the function $F(a, \lambda, \beta), \frac{a}{\lambda} = 0.08$, (b).

for all slow wave systems, but for DLW it is sharpened by relatively large a value, required to obtain the required β_g value. It is one of the restricting factors for DLW application in FW mode at low particles velocity. In Fig. 5 are shown the plots of the maximal (with respect to θ) $E_0, n = 0$ values for $P_t = 1MW, \beta_g = const = 0.01$, Fig. 5a, and the corresponding plots of E_{smax}/E_0 ratio, Fig. 5b. The iris thickness t in DLW cells should be as

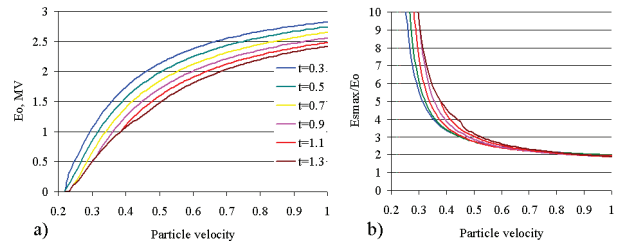


Figure 5: The plots of the maximal E_0 values for $P_t = 1MW, \beta_g = 0.01$ (a) and plots of E_{smax}/E_0 ratio, (b)

minimal, as it is possible from mechanical rigidity and heat transfer requirements. As one can see from Fig. 5a, for thin iris we can obtain higher E_0 value even with E_{smax} decreasing, Fig. 5b. With the thinner iris we obtain the required β_g value with smaller aperture radius a . It results

in E_0 increasing and also compensates partially E_{smax} increasing due to smaller t . For medium and low β values the strong dependence of the field decay, (4) emphasizes E_{smax} decreasing even for small a reduction. Also with t reduction slightly increases the Q factor of the cell and decreases attenuation α . Totally it leads to the higher energy gain δW for DLW section. These considerations and conclusion are also valid for BW $n = -1$ operating mode.

In Fig. 6 are shown obtained in the numerical results

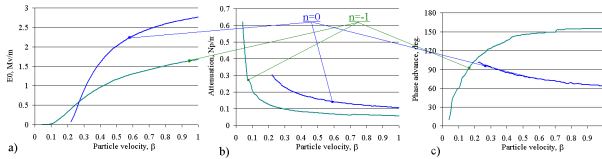


Figure 6: The plots of the maximal E_0 and E_{-1} values assuming $Pt = 1MW, |\beta_g| = 0.01$, (a), corresponding plots of attenuation α , (b), and optimal phase advance θ , (c) for FW $n = 0$ and BW $n = -1$ operation.

treatment the plots of the maximal E_0 and E_{-1} values, $Pt = 1MW, |\beta_g| = 0.01$, Fig. 6a, corresponding plots of attenuation α , Fig. 6b, and optimal phase advance θ , Fig. 6c both for FW $n = 0$ and BW $n = -1$ operation. A one can see, the plot $E_0(\beta)$ in Fig. 6a is very similar to the plot of the function $F(a, \lambda, \beta)$ in Fig. 4b. But in the range $0.1 \leq \beta \leq 0.25$ operation with $n = -1$ spatial harmonic allows higher accelerating gradient than for classical $n = 0$ case. In this region also attenuation α is essentially lower, Fig. 6b, for BW operation. It indicates, that for possible DLW application in the range $0.1 \leq \beta \leq 0.35$ BW operating mode is preferable. But DLW application in this range is at the expense of RF power and can be considered for specific purposes, [4].

DLW SECTION DESIGN

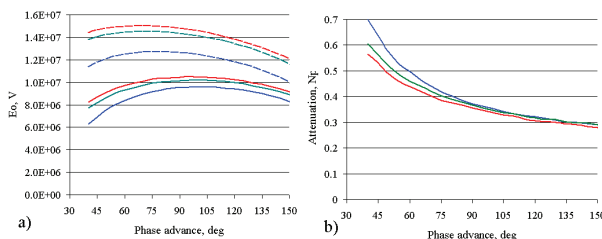


Figure 7: For constant gradient DLW sections (see text), the maximal possible E_0 (dotted curves) and realized E_0 (solid curves) values, attenuation α , (b).

The maximal value of accelerating gradient, which can be obtained for the fixed RF power depends on θ, β and β_g values. These dependencies are shown in plots on Fig. 6c for the single DLW cell. With application at moderate β the length of the DLW cell d_p should follow to the particle

velocity β and the constant gradient DLW option is reasonable. This case each section has the input and output β_g values, β_{gin}, β_{gou} . In Fig. 7a with dotted lines are shown plots $E_0(\theta)$ for input particle velocity $\beta_{in} = 0.56$, (blue), $\beta_{in} = 0.79$, (green) and $\beta_{in} = 0.89$, (red curves), assuming $\beta_g = 0.6\%, Pt = 18MW, n = 0, f_0 = 1296MHz$. With solid lines in Fig. 7a are shown plots of $E_0(\theta)$, realized in DLW sections with the length $L \sim 2.5m, \sim 3.17m, \sim 3.3m$ for the same β_{in} and P_t values, assuming $\beta_{gou} = 0.6\%$. The maximal E_0 values shift to higher θ . If we select lower θ in the section beginning, near RF input, shorter cells with lower Q and higher attenuation α , Fig. 7b. To compensate larger wave attenuation, we have shorter cells and should change β_g along the section faster. For the same β_{gou} value, it results in larger β_{gin} and related E_0 reduction. To the section end with lower β_g the wave comes already more attenuated and better DLW performance for higher β are less realized. The shift between maximal E_0 values on dotted and solid lines in Fig. 7a depends on the total attenuation τ in the section. The maximum of the realized E_0 value is smooth enough and the relative difference in δW is several percents. But there is the essential difference in the number of cells in the section for higher θ , leading to cost reduction in construction and tuning.

The similar reasons for BW $n = -1$ operation fix the optimal θ value near 135° . Due to lower attenuation $\alpha, n = -1$ operating mode for DLW sections is more effective, as compared to $n = 0$, in wider β range, $\sim (0.3 \div 0.4)$. More details, explanations and design examples are given in [4].

SUMMARY

The limitation for DLW applications in very low β region comes from the fundamental effect - field decay in the aperture. But, starting from $\beta \sim (0.1 - 0.15)$, the structure can be considered for some specific applications at the expense of an additional RF power. For the range $\beta \sim (0.1 \div 0.4)$ the structure should be realized with the backward wave operating mode - more effective as compared to the classical forward wave operation.

REFERENCES

- [1] G. Loew, R. Neal, Accelerating Structures, in Linear Accelerators, ed. P. Lapostolle, E. Septier, Amsterdam, 1970
- [2] M.I. Aizatsky et. al., High current electron linac for investigations in new methods of acceleration. Fizika plazmy, Nauka, v. 20, n. 7,8, p. 671, 1994 (in Russian).
- [3] V. Paramonov. The data library for accelerating structures development. Proc. of the 1996 LINAC Conference, Geneva, CERN, v.2, p. 493, <http://www.JACoW.org>, 1996
- [4] V. Paramonov. Parameters of the Disk Loaded Waveguide structure for intermediate particles acceleration in the intermediate energy range. <http://www.arXiv.org>, :1307.6506v1, [physics.acc.ph], 2013.